Edith Cowan University

Research Online

Research outputs 2014 to 2021

3-2017

2D transition metal dichalcogenides and graphene-based ternary composites for photocatalytic hydrogen evolution and pollutants degradation

Ying Chen

Hongqi Sun
Edith Cowan University

Wenchao Peng

Follow this and additional works at: https://ro.ecu.edu.au/ecuworkspost2013

 Part of the Engineering Commons

10.3390/nano7030062
Chen, Y., Sun, H., & Peng, W. (2017). 2D transition metal dichalcogenides and graphene-based ternary composites for photocatalytic hydrogen evolution and pollutants degradation. *Nanomaterials*, *7*(3), Article 62.
https://doi.org/10.3390/nano7030062
This Journal Article is posted at Research Online.
https://ro.ecu.edu.au/ecuworkspost2013/2764

nanomaterials

MDPI

Review

2D Transition Metal Dichalcogenides and Graphene-Based Ternary Composites for Photocatalytic Hydrogen Evolution and Pollutants Degradation

Ying Chen [1,3], Hongqi Sun [2,*] and Wenchao Peng [1,*]

1 School of Chemical Engineering and Technology, Tianjin University, Tianjin 300072, China; yingchen@tju.edu.cn
2 School of Engineering, Edith Cowan University, 270 Joondalup Drive, Joondalup, Perth, WA 6027, Australia
3 Department of Chemical Engineering, Renai College of Tianjin University, Tianjin 301636, China
* Correspondence: h.sun@ecu.edu.au (H.S.); wenchao.peng@tju.edu.cn (W.P.); Tel.: +86-22-85356119 (W.P.)

Academic Editor: Hermenegildo García
Received: 26 January 2017; Accepted: 8 March 2017; Published: 15 March 2017

Abstract: Photocatalysis have attracted great attention due to their useful applications for sustainable hydrogen evolution and pollutants degradation. Transition metal dichalcogenides (TMDs) such as MoS_2 and WS_2 have exhibited great potential as cocatalysts to increase the photo-activity of some semiconductors. By combination with graphene (GR), enhanced cocatalysts of TMD/GR hybrids could be synthesized. GR here can act as a conductive electron channel for the transport of the photogenerated electrons, while the TMDs nanosheets in the hybrids can collect electrons and act as active sites for photocatalytic reactions. This mini review will focus on the application of TMD/GR hybrids as cocatalysts for semiconductors in photocatalytic reactions, by which we hope to provide enriched information of TMD/GR as a platform to develop more efficient photocatalysts for solar energy utilization.

Keywords: transition metal dichalcogenides (TMDs); graphene; photocatalytic; hydrogen evolution; pollutants degradation

1. Introduction

Since the discovery of the photocatalytic splitting of water on TiO_2 electrodes by Fujishima and Honda in 1972 [1], photocatalysis has attracted great attention for eliminating hazardous pollutants and generating sustainable energy [2]. Semiconductors such as TiO_2, ZnO, CdS, etc. can act as photocatalysts for the utilization of solar energy [3]. They are however limited in real application by the rapid electron–hole recombination [4–6]. Noble metal cocatalysts are usually loaded to enhance the activity of the semiconductor photocatalysts [7]. However, these metals are rare and expensive to apply [8]. The development of highly active and low cost cocatalysts remains a great challenge in the field of photocatalysis.

Transition metal dichalcogenides (TMDs) such as MoS_2 and WS_2 have exhibited excellent activities as cocatalysts for the modification of semiconductors [8,9]. The properties of TMDs can be tailored according to their crystalline structure and the number and stacking sequence of their nanosheets [10–14]. By loading TMDs cocatalysts, semiconductor–semiconductor or metal–semiconductor junctions will form, and more interfaces could be created [15,16]. Charge separation and electron transport can therefore be enhanced, leading to the activity improvement [15]. Furthermore, many kinds of TMDs with different phases were reported to be active for the electrochemical hydrogen evolution reaction (HER), which stems from their exposed and

under-coordinated edge sites [17–19]. Therefore, loading the TMDs as cocatalysts for semiconductors could also lower the activation energy and overpotential for photocatalytic H_2 evolution [8]. On the other hand, TMDs have special 2D layered structure, and can be used as effective supports for anchor of semiconductor nanoparticles, which could reduce the mobility, provide more active sites, and avoid coalescence and agglomeration of the semiconductors [20–22]. Based on the above analysis, TMDs have shown great potential as substitute of noble metal cocatalysts for the synthesis of composite photocatalysts with high activity [8].

Graphene (GR) consists of a single layer and sp^2-hybridized carbon lattice with excellent electrical (200,000 $cm^2 \cdot V^{-1} \cdot s^{-1}$), thermal, and mechanical properties, and is a novel material that has emerged as a rapidly rising star in the field of material science [23]. The photocatalytic activity of semiconductors can be greatly increased by loading GR as cocatalyst, mainly owing to the effective separation of the electron–hole pairs [24,25].

By combining GR with TMDs, new hybrid cocatalysts could be synthesized with 2D layered structures. GR here can transport the photogenerated electrons rapidly, and the TMDs in the hybrids can accept electrons and act as active sites for H_2 evolution or radicals generation. This mini review will focus on the synthesis methods of TMD/GR-based photocatalysts and their applications for photocatalytic H_2 evolution and organic pollutants degradation. Based on this review, we hope to offer enriched information of TMD/GR as a platform to fabricate more efficient photocatalysts for solar energy utilization.

2. TMD/GR-Based Composites for Photocatalytic H_2 Evolution

TiO_2 is the most frequently used semiconductor for photocatalytic H_2 evolution, which can only absorb and utilize UV light due to its large band gap (3.2 eV) [26]. Xiang et al. synthesized ternary composites consisting of TiO_2 nanoparticles grown on the MoS_2/GR hybrid as enhanced photocatalysts for H_2 evolution (Figure 1) [25]. The TiO_2-MoS_2/GR composites were prepared using a two-step hydrothermal method. As shown in Figure 1, the TiO_2 nanoparticles were supported on the 2D MoS_2/GR hybrid uniformly with intimate contact. The electrons can therefore transfer rapidly from TiO_2 to the MoS_2/GR cocatalyst, and the charge recombination can therefore be suppressed. The activity of the ternary composites can be tuned by adjusting the GR percentage of MoS_2/GR cocatalysts and the percentage of the MoS_2/GR hybrid for the ternary photocatalysts. The optimized TiO_2-MoS_2/GR composite could obtain a high H_2 evolution rate of 165.3 $\mu mol \cdot h^{-1}$ and a quantum efficiency of 9.7% at 365 nm.

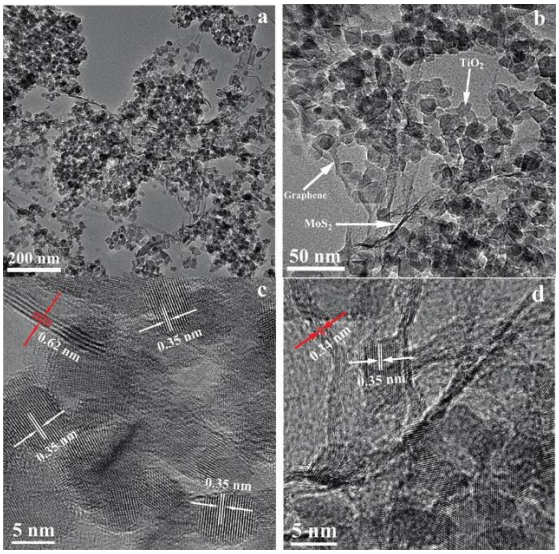


Figure 1. Morphology characterization of the TiO_2-MoS_2/graphene (GR) composite. (**a**,**b**) Transmission electron microscopy (TEM) and (**c**,**d**) high-resolution TEM (HRTEM) images of the TiO_2-MoS_2/GR composite (reprinted from [25] with permission, Copyright American Chemical Society, 2012).

CdS has a narrow bandgap of 2.3 eV, which is effective for capturing the visible light [36]. Chang et al. used nanosized GR as support for the growth of MoS_2; 3D hierarchical CdS-MoS_2/GR composites with diameters of 100–300 nm were then synthesized with the help of polyvinylpyrrolidone (PVP) (Figure 2) [27]. As shown in Figure 2e, the MoS_2 sheets on nanosized GR have many defect sites and disordered structures due to the low synthesis temperature, CdS nanoparticles can then firmly anchor on these defects and vacancies (Figure 2g–j). After optimizing each component proportion, the highest H_2 evolution rate could be as large as 1.8 mmol/h with an apparent quantum efficiency (AQE) of 28.1% at 420 nm, which was even higher than that of Pt/CdS. They thought that the activities of S atoms in the MoS_2 molecules were different with respect to their different coordination (Figure 3a). Unsaturated S atoms are active for H^+ adsorption and reduction (Figure 3b), while the saturated S atoms on the basal plane are inert. The nanosized few-layer MoS_2 supported on GR has more exposed edges and unsaturated active S atoms, which is therefore a promising cocatalyst for the activity enhancement of CdS.

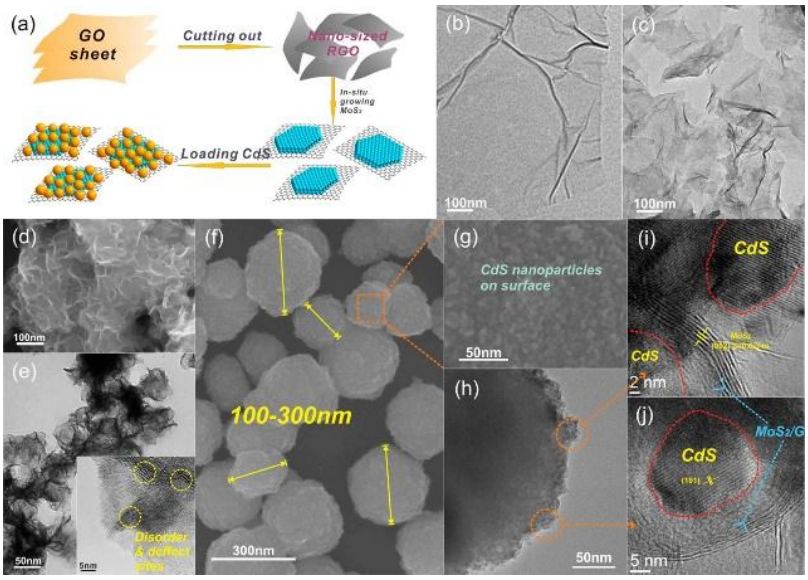


Figure 2. (**a**) Schematic illustration of growth mechanism of MoS_2/GR-CdS composites; TEM images of (**b**) graphene oxide (GO) and (**c**) nanosized graphene (GR); (**d**) Scanning electron microscopy (SEM) and (**e**) TEM images of as-prepared MoS_2/GR composite; the inset of (**e**) is the HRTEM image of MoS_2/GR composite; (**f** and **g**) SEM images of CdS-MoS_2/GR composites; (**h**) TEM and (**i** and **j**) HRTEM images of the CdS-MoS_2/GR composite (reprinted from [27] with permission, Copyright American Chemical Society, 2014).

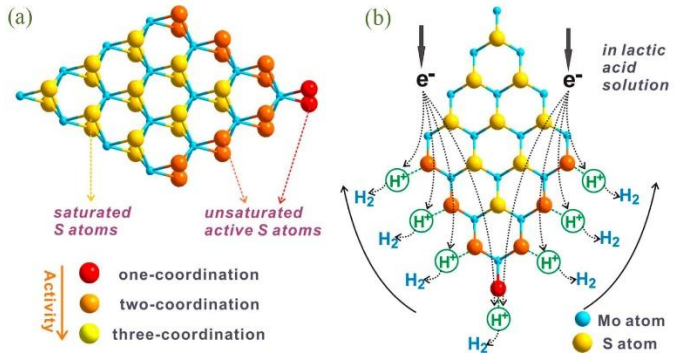


Figure 3. (**a**) Schematic illustration of the microstructure of MoS_2 and (**b**) its cocatalytic mechanism of H_2 generation in lactic acid solution (reprinted from [27] with permission, Copyright American Chemical Society, 2014).

Xiang et al. synthesized CdS-WS_2/GR ternary composites for photocatalytic H_2 evolution [32]. The optimized WS_2/GR content in the ternary CdS-WS_2/GR composites was determined to be 4.2 wt %. Using 0.35 M Na_2S/0.25 M Na_2SO_3 as sacrificial agent, a satisfactory H_2 evolution rate of 1.842 mmol·h^{-1}·g^{-1} could be achieved with an apparent quantum efficiency of 21.2% at 420 nm. The transient photocurrent response was also enhanced by loading the WS_2/GR cocatalyst, which was promising evidence for the improved charge transport (Figure 4). By loading WS_2/GR cocatalyst, more active sites will be introduced, and charge separation and interfacial charge transfer could be enhanced, thus leading to the greatly increased photo-activity.

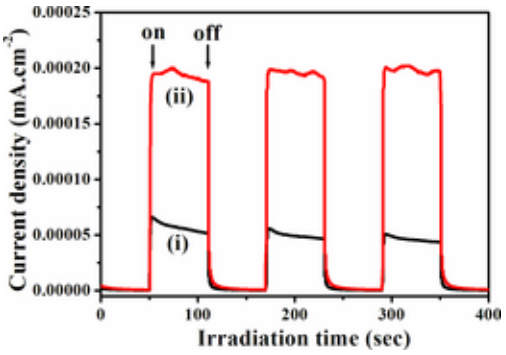


Figure 4. Transient photocurrent responses of pure CdS and CdS-WS_2/GR composite in 1 M Na_2SO_4 aqueous solution under visible-light irradiation at 0.5 V versus Ag/AgCl (reprinted from [32] with permission, Copyright Wiley-VCH, 2016).

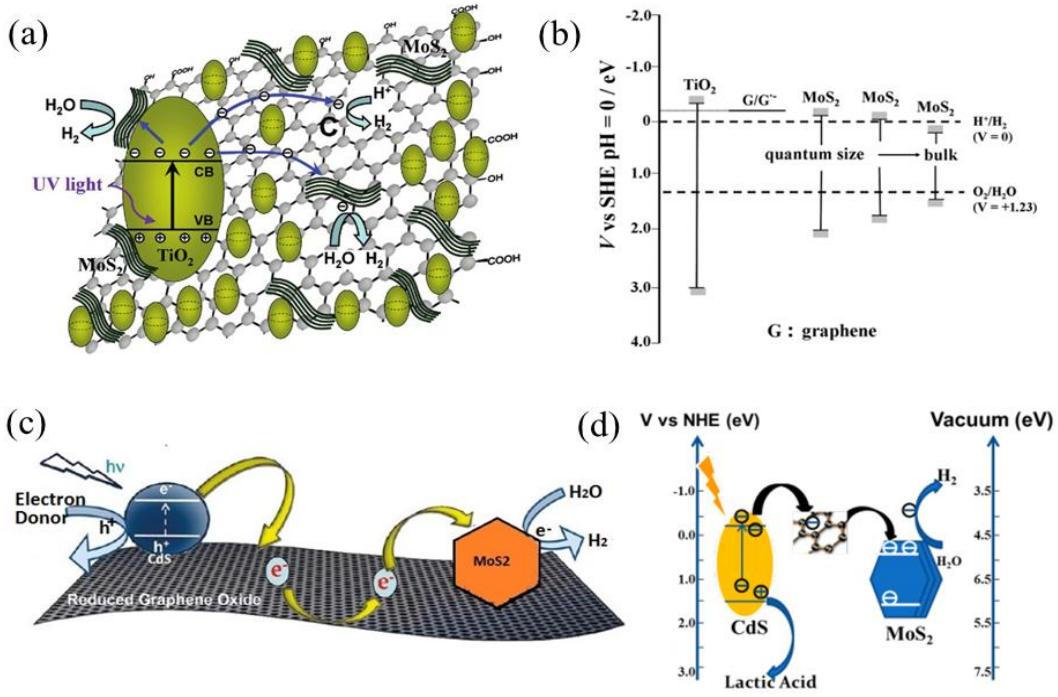


Figure 5. Schematic illustration of (**a**) the charge transfer in TiO_2-MoS_2/GR composites for photocatalytic H_2 evolution; and (**b**) the potential and band positions in the TiO_2/MoS_2/graphene system (reprinted from [25] with permission, Copyright American Chemical Society, 2012); (**c**) Graphene-supported CdS and MoS_2 for photocatalytic hydrogen evolution; (**d**) The band positions for the CdS–graphene–MoS_2 system (reprinted from [28] with permission, Copyright Royal Society of Chemistry, 2014). (SHE: Standard hydrogen electrode; NHE: Normal hydrogen electrode).

During the photocatalytic H_2 evolution process, the metal oxide can absorb a photon to create an electron–hole pair with irradiation (Figure 5a,c). Both of the graphene/ graphene$^{\bullet-}$ redox potential and conduction band (CB) of quantum-sized MoS_2 are slightly lower than the CB of anatase TiO_2 or CdS (Figure 4b,d). Part of the excited electrons can then directly transfer to active sites of MoS_2, and another part transfer to active sites of MoS_2 via graphene conducting channel. Graphene here can act as a "highway" for the rapid transport of photo-generated electrons, while MoS_2 nanosheets can accept electrons and act as active sites for H_2 evolution. Therefore, using MoS_2/GR hybrid as cocatalyst, suppression of charge recombination, improvement of interfacial charge transfer, and an increase in the number of active sites could be achieved, thus leading to the enhanced photo-activity.

It has been reported that sub-10 nm rutile TiO_2 with 1 wt % Pt doping exhibited state-of-the-art activity among TiO_2-based composites for photocatalytic water splitting. The hydrogen evolution rate could be achieved to 932 mmol·h^{-1}·g^{-1} under visible light (>400 nm) and 1954 mmol·h^{-1}·g^{-1} under simulated solar light [37]. By loading 0.30 wt % of Pt and 0.13 wt % of PdS as cocatalysts on CdS, another CdS-based state-of-the-art material could be synthesized with a quantum efficiency (QE) up to 93% and a hydrogen evolution rate of 8.77 mmol·h^{-1} [38]. Compared to these state-of-the-art materials, the activities of TMD/GR modified semiconductors are relatively weak, with lower H_2 evolution rates and QEs. Although the TMD/GR cocatalysts are more cost effective, deep studies are still needed to obtain higher efficiencies for real application.

3. TMD/GR-Based Photocatalysts for Pollutants Degradation

Photocatalysis is also an attractive technology for the degradation of pollutants in water using solar energy [39]. Han et al. used a hydrothermal method to combine the exfoliated MoS_2, GR, and TiO_2 P25 together [40]. The obtained composite was a novel graphene-based three-dimensional (3D) aerogel embedded with TiO_2 particles and MoS_2 nanosheets (Figure 6). Porous structure could be observed with pore sizes of about several micrometers (Figure 6b). The Nyquist plots of the samples were also tested, and the final 3D GR–MoS_2–TiO_2 composite had the smallest cure radius (Figure 7), indicating that the addition of 3D graphene aerogel can decrease the solid state interface layer resistance and the charge transfer resistance. During the application test, the final composite had better adsorption ability for methyl orange (MO) due to the maximization of accessible sites of the 3D interconnected networks (Figure 8a). The 3D photocatalyst was proved to be very effective for the photocatalytic degradation of MO, and nearly no MO was left after 15 min irradiation (Figure 8b).

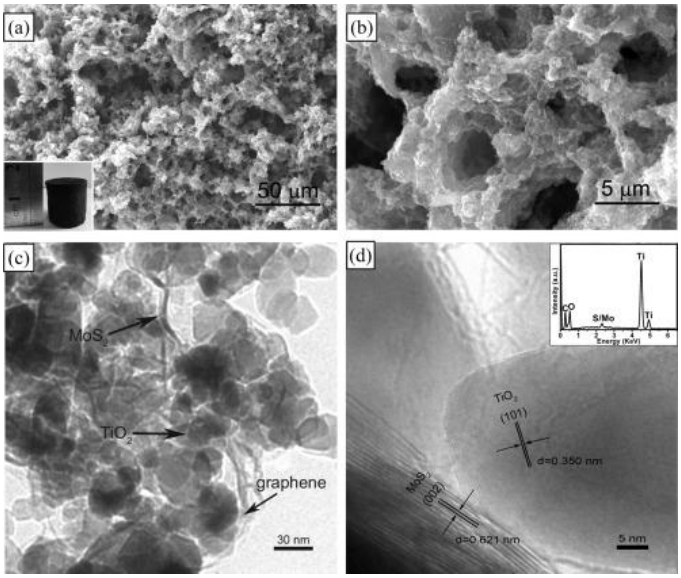


Figure 6. (**a**,**b**) SEM images of the as-prepared MoS_2/P25/GR-aerogel; the inset image is a digital photo of the free-standing MoS_2/P25/GR-aerogel. (**c**,**d**) TEM images and energy-dispersive X-ray spectroscopy (EDS) (insert) pattern of the as-prepared MoS_2/P25/GR-aerogel (reprinted from [40] with permission, Copyright Elsevier, 2014).

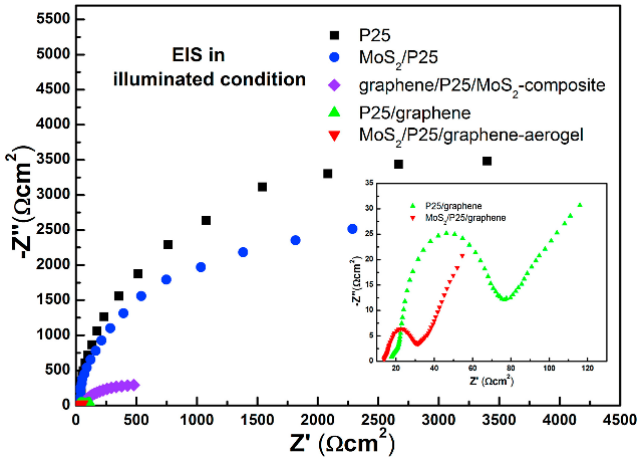


Figure 7. Electrochemical impedance spectroscopy (EIS) Nyquist plots of MoS_2/P25/GR-aerogel, GR/P25/MoS_2-composite, P25/GR, MoS_2/P25, and P25 nanoparticles in sulfide-sulfite electrolyte and under UV irradiation (reprinted from [40] with permission, Copyright Elsevier, 2014).

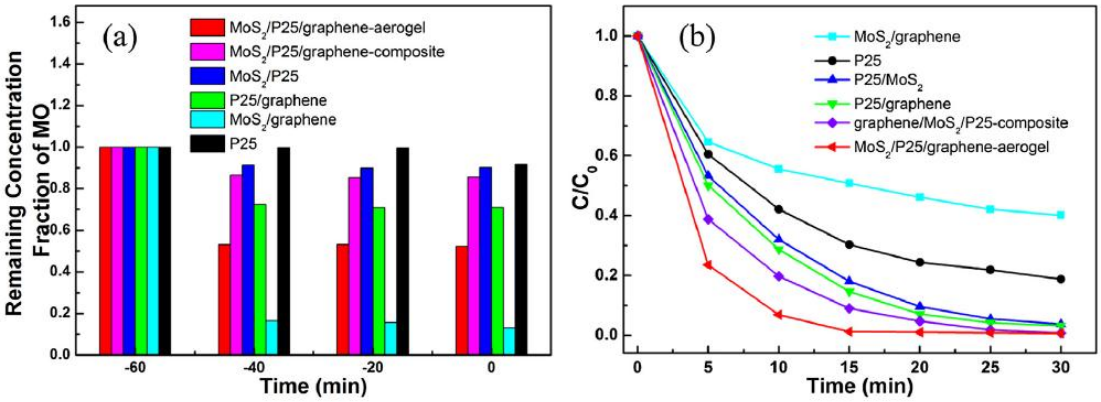


Figure 8. (**a**) Bar plot showing the remaining methyl orange (MO) in solution after reaching the adsorption equilibrium in the dark over MoS2/P25/GR-aerogel, GR/P25/MoS2-composite, P25/GR, MoS2/P25, MoS2/GR, and P25; (**b**) photo-degradation of MO by MoS2/P25/GR-aerogel, GR/P25/MoS2-composite, P25/GR, MoS2/P25, MoS2/GR, and P25 with a reaction time of 30 min under UV irradiation (reprinted from [40] with permission, Copyright Elsevier, 2014).

Gao et al. fabricated a TiO_2-MoS_2/GR composite under atmospheric pressure using a simple one-pot solvothermal method [34]. Na_2MoO_4 and thiocarbamide were used as precursors for MoS_2, and mixed solvent of (dimethylacetamide (DMAc)/deionized (DI) H_2O) was used as reaction media. Under the above conditions, MoS_2 quantum dots (QDs) with (100) face exposed could be generated on the surface of TiO_2 and GR (Figure 9). Attributed to the small diameter of the MoS_2 QDs, more active edge could be created, thus leading to the enhanced photocatalytic activity.

Peng et al. synthesized Ag_3PO_4-MoS_2/GR via a simple two-step hydrothermal process [33]. The composite was found to be an effective catalyst for the photo-decomposition of 2,4-dichlorophenol (DCP) under simulated solar light and visible light ($\lambda > 420$ nm). They described the major reaction steps involved in this photocatalytic process as follows:

$$Ag_3PO_4 + hv \rightarrow Ag_3PO_4\ (e^- + h^+) \quad (1)$$

$$Ag_3PO_4\ (e^-) + MoS_2/GR \rightarrow Ag_3PO_4 + MoS_2/GR\ (e^-) \quad (2)$$

$$MoS_2/GR\ (e^-) + O_2 \rightarrow MoS_2/GR + O_2{}^- \quad (3)$$

$$Ag_3PO_4\ (h^+) + DCP \rightarrow CO_2 + H_2O + \text{other products} \quad (4)$$

$$Ag_3PO_4\ (h^+) + OH^- \rightarrow Ag_3PO_4 + \cdot OH \quad (5)$$

$$\cdot OH + DCP \rightarrow CO_2 + H_2O + \text{other products} \quad (6)$$

As shown in the mechanism, electrons and holes could be separated with irradiation (1). The holes could oxidize the DCP molecules adsorbed on the catalyst surface directly (4). They could also react with water (or hydroxyl) to form hydroxyl free radicals (·OH), which are strong oxidants for DCP decomposition (5). The MoS_2/GR cocatalyst here could act as electron collectors to facilitate the interfacial electron transfer and charge separation. In addition, the MoS_2/GR cocatalyst could also provide more active sites and allow for the activation of dissolved O_2 for organic degradation [33].

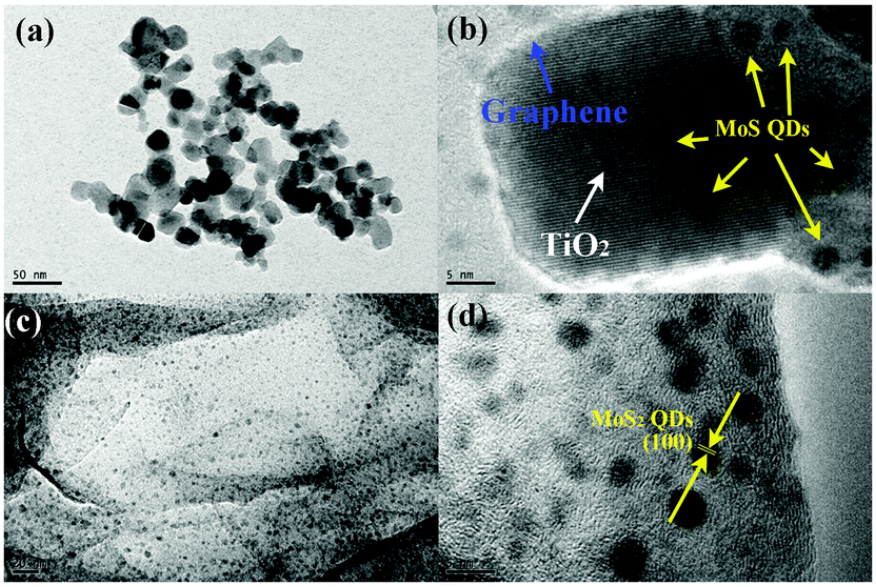


Figure 9. TEM and HRTEM images of the sample (**a**,**b**) TiO_2-MoS_2/GR and (**c**,**d**) MoS_2–GR (reprinted from [34] with permission, Copyright Royal Society of Chemistry, 2015). QD: quantum dot.

Using CoS_2/GR as cocatalyst, Zhu et al. supported TiO_2 nanoparticles on its surface using a facile sonochemical and hydrothermal method [35]. Their photo-activity was then evaluated for the degradation of methylene blue (MB) and Texbrite BA-L (TBA) under visible light. Enhanced activity was obtained due to the synergetic effect between TiO_2 and the CoS_2/GR cocatalyst. The recent progress of TMD/GR based photocatalysts for H_2 evolution and pollutants degradation are summarized and shown in Table 1 for a easier perusal.

Table 1. Summary of transition metal dichalcogenides (TMD)/GR based photocatalysts and their applications.

Catalyst	Synthesis Method	Application	Light Source	Activity	Morphology	Ref.
TiO_2-MoS_2/GR	Two-step hydrothermal	H_2 generation in 25% (v/v) ethanol/water	350 W Xe arc lamp 20 mW/cm^{-2} λ = 365 nm	165.3 μmol·h^{-1} [a] QE: 9.7% at 365 nm	Particles/sheets	[25]
CdS-MoS_2/GR	Hydrothermal	H_2 generation in 20 vol % lactic solution	300 W Xe lamp (λ > 420 nm)	1.8 mmol/h QE: 28.1% at 420 nm	Particles/sheets	[27]
CdS-MoS_2/GR	Sonication assisted post loading	H_2 generation in 10 vol % lactic acid	500 W UV-vis lamp	3.067 mL·h^{-1}	Particles/sheets	[28]
CdS-MoS_2/GR	In-situ photo deposition	H_2 generation in 10 vol % lactic acid	350 W Xe lamp $\lambda \geq$ 420 nm 34 mW/cm^2	99 μmol·h^{-1} QE: 9.8% at 420 nm	Particles/sheets	[29]
ZnS-MoS_2/GR	One-pot hydrothermal	H_2 generation in 0.005 M Na_2S and 0.005 M Na_2SO_3	300 W Xe lamp 125 mW/cm^2	2258 μmol·h^{-1}·g^{-1}	Particles/sheets	[30]
CdS-MoS_2/GR	Two-step solvothermal	H_2 generation in 10 vol % lactic acid	350 W xenon arc lamp ($\lambda \geq$ 420 nm)	621.3 μmol·h^{-1} 54.4% at 420 nm	Nanorods /sheets	[31]
CdS-WS_2/GR	Solvothermal	H_2 generation in 0.35 M Na_2S and 0.25 M Na_2SO_3	500 W Xeno arc Lamp λ > 420 nm	1842 μmol·h^{-1}·g^{-1} 21.2% at 420 nm	Nanosheets/nanorods	[32]
Ag_3PO_4-MoS_2/GR	Hydrothermal-deposition	2,4-Dichlorophenol degradation 20 mg·L^{-1}	500 W xenon lamp (λ > 420 nm)	[b] DP of >99% in 20 min 25 times higher than N-TiO_2	Sub-microcrystal/sheets	[33]
TiO_2-MoS_2/GR	One-pot solvothermal	RhB degradation 10 mg·L^{-1}	150 W Xe lamp	DP of 80% in 80 min 3.9 times higher than TiO_2 P25	Sheets/Particles	[34]
TiO_2-CoS_2/GR	Sonochemical and hydrothermal method	MB degradation 2.0×10^{-5} mol/L	8 W, halogen lamp 400–790 nm.	DP of >90% in 90 min	Sheets/Particles	[35]

[a] QE: Quantum efficiency; [b] DP: Degradation percentage.

4. Conclusions and Perspective

This mini review focused on the recent developments of the TMD/GR-based composites, including the synthesis methods, the application in photocatalytic H_2 evolution, and the application for organic pollutants degradation. By combination with GR, the TMD/GR hybrids were more effective as cocatalysts for the modification of semiconductors. GR here can act as a conductive electron transport "highway" for the transport of the photogenerated electrons, and the TMDs nanosheets in the hybrids can accept electrons and act as active sites for photocatalytic reactions. Although deep research is still needed for real application, TMD/GR cocatalysts have shown great potential as a platform to fabricate more efficient photocatalysts for solar energy utilization.

Acknowledgments: This research was supported by the project No. 21506158 from the National Natural Science Foundation of China (NSFC).

Conflicts of Interest: The authors declare no conflict of interest.

References

1. Inoue, T.; Fujishima, A.; Konishi, S.; Honda, K. Photoelectrocatalytic Reduction of Carbon Dioxide in Aqueous Suspensions of Semiconductor Powders. *Nature* **1979**, *277*, 637–638. [CrossRef]
2. Rajeshwar, K.; De Tacconi, N.R. Solution Combustion Synthesis of Oxide Semiconductors for Solar Energy Conversion and Environmental Remediation. *Chem. Soc. Rev.* **2009**, *7*, 1984–1998. [CrossRef] [PubMed]
3. Kudo, A.; Miseki, Y. Heterogeneous Photocatalyst Materials for Water Splitting. *Chem. Soc. Rev.* **2009**, *1*, 253–278. [CrossRef] [PubMed]
4. Perera, S.D.; Mariano, R.G.; Vu, K.; Nour, N.; Seitz, O.; Chabal, Y.; Balkus, K.J. Hydrothermal Synthesis of Graphene-TiO_2 Nanotube Composites with Enhanced Photocatalytic Activity. *Acs. Catal.* **2012**, *6*, 949–956. [CrossRef]
5. Li, P.; Wei, Z.; Wu, T.; Peng, Q.; Li, Y.D. Au-Zno Hybrid Nanopyramids and Their Photocatalytic Properties. *J. Am. Chem. Soc.* **2011**, *15*, 5660–5663. [CrossRef]
6. Liu, Y.; Yu, Y.X.; Zhang, W.D. MoS_2/CdS Heterojunction with High Photoelectrochemical Activity for H_2 Evolution under Visible Light: The Role of MoS_2. *J. Phys. Chem. C* **2013**, *25*, 12949–12957. [CrossRef]
7. Zou, X.X.; Zhang, Y. Noble Metal-Free Hydrogen Evolution Catalysts for Water Splitting. *Chem. Soc. Rev.* **2015**, *15*, 5148–5180. [CrossRef] [PubMed]
8. Lu, Q.P.; Yu, Y.F.; Ma, Q.L.; Chen, B.; Zhang, H. 2D Transition-Metal-Dichalcogenide-Nanosheet-Based Composites for Photocatalytic and Electrocatalytic Hydrogen Evolution Reactions. *Adv. Mater.* **2016**, *10*, 1917–1933. [CrossRef] [PubMed]
9. Chang, K.; Hai, X.; Ye, J.H. Transition Metal Disulfides as Noble-Metal-Alternative Co-Catalysts for Solar Hydrogen Production. *Adv. Energy Mater.* **2016**, *10*. [CrossRef]
10. Bhandavat, R.; David, L.; Singh, G. Synthesis of Surface-Functionalized WS_2 nanosheets and Performance as Li-Ion Battery Anodes. *J. Phys. Chem. Lett.* **2012**, *11*, 1523–1530. [CrossRef] [PubMed]
11. Gong, Q.F.; Cheng, L.; Liu, C.H.; Zhang, M.; Feng, Q.L.; Ye, H.L.; Zeng, M.; Xie, L.M.; Liu, Z.; Li, Y.G. Ultrathin $MoS_{2(1-x)}Se_{2x}$ alloy Nanoflakes for Electrocatalytic Hydrogen Evolution Reaction. *ACS Catal.* **2015**, *4*, 2213–2219. [CrossRef]
12. Prabakaran, A.; Dillon, F.; Melbourne, J.; Jones, L.; Nicholls, R.J.; Holdway, P.; Britton, J.; Koos, A.A.; Crossley, A.; Nellist, P.D.; et al. WS_2 2D Nanosheets in 3D Nanoflowers. *Chem. Commun. (Camb.)* **2014**, *82*, 12360–12362. [CrossRef] [PubMed]
13. Lee, S.C.; Benck, J.D.; Tsai, C.; Park, J.; Koh, A.L.; Abild-Pedersen, F.; Jaramillo, T.F.; Sinclair, R. Chemical and Phase Evolution of Amorphous Molybdenum Sulfide Catalysts for Electrochemical Hydrogen Production. *ACS NANO* **2016**, *1*, 624–632. [CrossRef] [PubMed]
14. Baldovi, H.G.; Latorre-Sanchez, M.; Esteve-Adell, I.; Khan, A.; Asiri, A.M.; Kosa, S.A.; Garcia, H. Generation of MoS_2 Quantum Dots by Laser Ablation of MoS_2 Particles in Suspension and Their Photocatalytic Activity for H_2 Generation. *J. Nanoparticle Res.* **2016**, *8*, 240. [CrossRef]
15. Zong, X.; Yan, H.J.; Wu, G.P.; Ma, G.J.; Wen, F.Y.; Wang, L.; Li, C. Enhancement of Photocatalytic H_2 Evolution on CdS by Loading MoS_2 as Cocatalyst under Visible Light Irradiation. *J. Am. Chem. Soc.* **2008**, *23*, 7176–7177. [CrossRef] [PubMed]

16. Bai, S.; Wang, L.M.; Chen, X.Y.; Du, J.T.; Xiong, Y.J. Chemically exfoliated metallic MoS_2 nanosheets: A promising supporting Co-catalyst for enhancing the photocatalytic performance of TiO_2 nanocrystals. *Nano Res.* **2015**, *1*, 175–183. [CrossRef]
17. Morales-Guio, C.G.; Stern, L.A.; Hu, X.L. Nanostructured hydrotreating catalysts for electrochemical hydrogen evolution. *Chem. Soc. Rev.* **2014**, *18*, 6555–6569. [CrossRef] [PubMed]
18. Morales-Guio, C.G.; Hu, X.L. Amorphous molybdenum sulfides as hydrogen evolution catalysts. *Accounts Chem. Res.* **2014**, *8*, 2671–2681. [CrossRef] [PubMed]
19. Yan, Y.; Xia, B.Y.; Xu, Z.C.; Wang, X. Recent development of molybdenum sulfides as advanced electrocatalysts for hydrogen evolution reaction. *Acs Catal.* **2014**, *6*, 1693–1705. [CrossRef]
20. Zhang, J.; Zhu, Z.P.; Feng, X.L. Construction of two-dimensional MoS_2/CdS p-n nanohybrids for highly efficient photocatalytic hydrogen evolution. *Chem.-A Eur. J.* **2014**, *34*, 10632–10635. [CrossRef] [PubMed]
21. Zhu, Y.Y.; Ling, Q.; Liu, Y.F.; Wang, H.; Zhu, Y.F. Photocatalytic H_2 evolution on MoS_2-TiO_2 catalysts synthesized via mechanochemistry. *Phys. Chem. Chem. Phys.* **2015**, *2*, 933–940. [CrossRef] [PubMed]
22. Vattikuti, S.P.; Byon, C.; Reddy, C.V.; Ravikumar, R.V. Improved photocatalytic activity of MoS_2 nanosheets decorated with SnO_2 nanoparticles. *Rsc Adv.* **2015**, *105*, 86675–86684. [CrossRef]
23. Novoselov, K.S.; Geim, A.K.; Morozov, S.V.; Jiang, D.; Zhang, Y.; Dubonos, S.V.; Grigorieva, I.V.; Firsov, A.A. Electric field effect in atomically thin carbon films. *Science* **2004**, *5696*, 666–669. [CrossRef] [PubMed]
24. Peng, W.C.; Li, X.Y. Synthesis of a sulfur-graphene composite as an enhanced metal-free photocatalyst. *Nano Res.* **2013**, *4*, 286–292. [CrossRef]
25. Xiang, Q.J.; Yu, J.G.; Jaroniec, M. Synergetic effect of MoS_2 and graphene as cocatalysts for enhanced photocatalytic H_2 production activity of TiO_2 nanoparticles. *J. Am. Chem. Soc.* **2012**, *15*, 6575–6578. [CrossRef] [PubMed]
26. Liu, G.; Zhao, Y.; Sun, C.; Li, F.; Lu, G.Q.; Cheng, H.-M. Synergistic effects of B/N doping on the visible-light photocatalytic activity of mesoporous TiO_2. *Angew. Chem.-Int. Ed.* **2008**, *24*, 4516–4520. [CrossRef] [PubMed]
27. Chang, K.; Mei, Z.W.; Wang, T.; Kang, Q.; Ouyang, S.X.; Ye, J.H. MoS_2/graphene cocatalyst for efficient photocatalytic h_2 evolution under visible light irradiation. *Acs NANO* **2014**, *7*, 7078–7087. [CrossRef] [PubMed]
28. Jia, T.T.; Kolpin, A.; Ma, C.S.; Chan, R.C.T.; Kwok, W.M.; Tsang, S.C.E. A Graphene dispersed CdS-MoS_2 nanocrystal ensemble for cooperative photocatalytic hydrogen production from water. *Chem. Commun.* **2014**, *10*, 1185–1188. [CrossRef] [PubMed]
29. Li, Y.X.; Wang, H.; Peng, S.Q. Tunable Photodeposition of MoS_2 onto a Composite of Reduced Graphene Oxide and Cds for Synergic Photocatalytic Hydrogen Generation. *J. Phys. Chem. C* **2014**, *34*, 19842–19848. [CrossRef]
30. Zhu, B.L.; Lin, B.Z.; Zhou, Y.; Sun, P.; Yao, Q.R.; Chen, Y.L.; Gao, B.F. Enhanced photocatalytic H_2 evolution on Zns loaded with graphene and MoS_2 nanosheets as cocatalysts. *J. Mater. Chem. A* **2014**, *11*, 3819–3827. [CrossRef]
31. Lang, D.; Shen, T.T.; Xiang, Q.J. Roles of MoS_2 and graphene as cocatalysts in the enhanced visible-light photocatalytic H_2 production activity of multiarmed CdS nanorods. *Chemcatchem* **2015**, *6*, 943–951. [CrossRef]
32. Xiang, Q.J.; Cheng, F.Y.; Lang, D. Hierarchical layered WS_2/graphene-modified CdS nanorods for efficient photocatalytic hydrogen evolution. *Chemsuschem* **2016**, *9*, 996–1002. [CrossRef] [PubMed]
33. Peng, W.C.; Wang, X.; Li, X.Y. The synergetic effect of MoS_2 and graphene on Ag_3PO_4 for its ultra-enhanced photocatalytic activity in phenol degradation under visible light. *Nanoscale* **2014**, *14*, 8311–8317. [CrossRef] [PubMed]
34. Gao, W.Y.; Wang, M.Q.; Ran, C.X.; Li, L. Facile one-pot synthesis of MoS_2 quantum dots-graphene-TiO_2 composites for highly enhanced photocatalytic properties. *Chem. Commun.* **2015**, *9*, 1709–1712. [CrossRef] [PubMed]
35. Zhu, L.; Jo, S.B.; Ye, S.; Ullah, K.; Meng, Z.D.; Oh, W.C. A Green and direct synthesis of photosensitized CoS_2-graphene/TiO_2 hybrid with high photocatalytic performance. *J. Ind. Eng. Chem.* **2015**, *22*, 264–271. [CrossRef]
36. Wang, G.M.; Yang, X.Y.; Qian, F.; Zhang, J.Z.; Li, Y. Double-sided cds and cdse quantum dot co-sensitized ZnO nanowire arrays for photoelectrochemical hydrogen generation. *NANO Lett.* **2010**, *3*, 1088–1092. [CrossRef] [PubMed]

37. Li, L.; Yan, J.; Wang, T.; Zhao, Z.-J.; Zhang, J.; Gong, J.; Guan, N. Sub-10 nm rutile titanium dioxide nanoparticles for efficient visible-light-driven photocatalytic hydrogen production. *Nat. Commun.* **2015**, *6*. [CrossRef] [PubMed]
38. Yan, H.; Yang, J.; Ma, G.; Wu, G.; Zong, X.; Lei, Z.; Shi, J.; Li, C. Visible-light-driven hydrogen production with extremely high quantum efficiency on Pt-PdS/CdS photocatalyst. *J. Catal.* **2009**, *2*, 165–168. [CrossRef]
39. Hoffmann, M.R.; Martin, S.T.; Choi, W.Y.; Bahnemann, D.W. Environmental applications of semiconductor photocatalysis. *Chem. Rev.* **1995**, *1*, 69–96. [CrossRef]
40. Han, W.J.; Zang, C.; Huang, Z.Y.; Zhang, H.; Ren, L.; Qi, X.; Zhong, J.X. Enhanced photocatalytic activities of three-dimensional graphene-based aerogel embedding TiO_2 nanoparticles and loading MoS_2 nanosheets as Co-catalyst. *Int. J. Hydrog. Energy* **2014**, *34*, 19502–19512. [CrossRef]



© 2017 by the authors. Licensee MDPI, Basel, Switzerland. This article is an open access article distributed under the terms and conditions of the Creative Commons Attribution (CC BY) license (http://creativecommons.org/licenses/by/4.0/).